Saudi Journal of Biological Sciences 27 (2020) 3025–3034

Contents lists available at ScienceDirect

Saudi Journal of Biological Sciences

journal homepage: www.sciencedirect.com

Original article

Phytochemical profiling, antioxidant and antiproliferation potential of *Euphorbia milii* var.: Experimental analysis and in-silico validation

Talha Ali Chohan [a,1], Muhammad Sarfraz [b,1], Kanwal Rehman [d], Tariq Muhammad [c], Muhammad Usman Ghori [e], Kashif Maqbool Khan [f], Iftikhar Afzal [g], Muhammad Sajid Hamid Akash [h], Alamgeer [i], Arif Malik [a], Tahir Ali Chohan [f,*]

[a] Institute of Molecular Biology and Biotechnology, The University of Lahore, Pakistan
[b] College of Pharmacy, Al Ain University, Al Ain Campus, United Arab Emirates
[c] Department of Pharmacology, Lahore Pharmacy College, Lahore, Pakistan
[d] Department of Pharmacy, University of Agriculture, Faisalabad, Pakistan
[e] Department of Pharmacy, School of Applied Sciences, University of Huddersfield, Huddersfield, UK
[f] Laboratory of Natural Products and Computational Chemistry, Institute of Pharmaceutical Sciences, University of Veterinary and Animal Sciences, Lahore, Pakistan
[g] Department of Pharmaceutical Chemistry, Faculty of Pharmacy, University of Sargodha, Pakistan
[h] Department of Pharmaceutical Chemistry, Government College University, Faisalabad, Pakistan
[i] Punjab University College of Pharmacy, University of the Punjab, Lahore, Pakistan

ARTICLE INFO

Article history:
Received 31 March 2020
Revised 27 July 2020
Accepted 1 August 2020
Available online 6 August 2020

Keywords:
Cytotoxicity
Antioxidant
Phytochemicals
MD simulation
Molecular docking

ABSTRACT

This study was aimed to investigate the anticancer potential of *Euphorbia milii* (*E. milii*) using an exquisite combination of phytopharmacological and advanced computational techniques. The chloroform fraction (Em-C) of *E. milii* methanol extract showed the highest antioxidant activity (IC_{50}: 6.41 ± 0.99 μg/ml) among all studied fractions. Likewise, Em-C also showed significant cytotoxicity (IC_{50}: 11.2 ± 0.8 μg/ml) when compared with that of standard compound 5-fluorouracil (5-FU) (IC_{50}: 4.22 ± 0.6 μg/ml) against hepatocarcinoma cell line (HepG2). However, in a human cervical cancer cell line (HeLa), Em-C demonstrated a non-significant difference in cytotoxicity (22.1 ± 0.8 μg/ml) when compared with that of 5-FU (IC_{50}: 6.87 ± 0.5 μg/ml). Furthermore, Western blot and qRT-PCR analysis revealed that the suppression of HepG2 cells was the consequence of a tremendous decrease in CDK2 and E2F1 protein expression. The GC–MS analysis of Em-C revealed the unique presence of cyclobarbital (CBT) and benzodioxole derivative (BAN) as major constituents. Furthermore, molecular docking of compounds BAN, CBT, and MBT into the binding site of different molecular targets i.e. cyclin dependent kinase 2 (CDK2), thymidylate synthase (TS), caspase 3, BCL2 and topoisomerase II was carried out. Compounds BAN and CBT have demonstrated remarkable binding affinity towards CDK2 and thymidylate synthase, respectively. Molecular dynamic simulation studies have further confirmed the finding of docking analysis, suggesting that CDK2 and TS can act as an attractive molecular target for BAN and CBT, respectively. It can be concluded that these *E. milii* phytoconstituents (BAN and CBT) may likely be responsible for anti-invasive activity against HepG2 cells.

1. Introduction

Cancer has been ranked as the second leading cause of mortality worldwide, accounting for more than nine miliion causalities during the last year (Bray et al., 2018). Since several different factors may lead to malignancy; targeting cancer cells without harming normal cells has remained to be a challenging task for pharmaceutical scientists (Chohan et al., 2015). Conventional modalities such as surgical removal, hormonal therapy, immune therapy, radiotherapy and chemotherapy for cancer treatment has inadequate

* Corresponding author.
E-mail address: tahir.chohan@uvas.edu.pk (T.A. Chohan).
[1] Talha Ali Chohan and Muhammad Sarfraz has contributed equally in this manuscript.

Peer review under responsibility of King Saud University.

Production and hosting by Elsevier

https://doi.org/10.1016/j.sjbs.2020.08.003
1319-562X/

ability to discriminate between the normal and cancerous cells (Chohan et al., 2018); hence, causing unacceptable toxicities with modest therapeutic benefits. Alternatively, the natural products from plant kingdom offer protective and therapeutic actions to all cells with low cytotoxicity (Safarzadeh et al., 2014). Various renowned cytotoxic drugs, including Vinca alkaloids (from Catharanthus roseus), podophyllotoxin (from Podophyllum) and paclitaxel (from Taxus brevifolia) (Kumar et al., 2013) have been obtained from the plant kingdom. Apart from the considerable potential of Asian flora as a source of numerous cytotoxic agents (Kaur et al., 2011), only a few of these medicinal plants have been intensively investigated for their ability to cure malignancy; while, a large proportion of Asian flora has not been well studied (Saxena et al., 2013). Since the pharmacotherapeutic properties of medicinal plants are primarily attributed to the blend of various phytochemicals (Kaur et al., 2011), an intensive demonstration of cytotoxic potential of these partially explored medicinal plants and characterization of their bioactive phytochemicals may represent safer and alternative therapeutic intervention for cancer management.

The genus *Euphorbia* comprises one of the widespread genera of medicinal plants distributed throughout the tropical regions of Pakistan, India and China (Rauf et al., 2014). Due to substantial therapeutic potential, various species of *Euphorbia* are traditionally being implicated as a folk medicine for the treatment of different ailments such as warts, eczema and eradication of intestinal parasites (Bani et al., 2007; Chaman et al., 2019). The phytochemical profiling of various *Euphorbia* species had demonstrated the presence of a variety of bioactive secondary metabolites including vitexicarpin, daucosterol, artemetin, p-hyfroxybenzoic acid, diterpenes (Chaman et al., 2019), euphorbetin, β-sitosterol, aesculetin, kaempferol-3-glucuronide, daphnetin (Zheng et al., 2009). *Euphorbia milii (E. milii)* also known as ‘‘crown of thorns” or ‘‘christ plant” is a seasonal bloom (Qaisar et al., 2012), included among the most renowned medicinal plants of this genus for their folklore implication as a remedy against skin infections, warts, cancer and liver disorder (Delgado et al., 2003). *E. milii* has also been reported to exhibit antifungal, antinociceptive and molluscicidal properties (Rauf et al., 2014). Furthermore, *E. milii* has been reported to possess various phytochemicals such as cycloartenol, amyrin acetate, triterpenes, lupeol acetate, flavonoids (Qaisar and Khawaja, 2012), and lectin (Tonoli et al., 2012).

Although, a plethora of evidence regarding the therapeutic efficacy of *E. milii* has been published (Rauf et al., 2014; Chaman et al., 2019; Qaisar and Khawaja, 2012), the knowledge of bioactive phytochemicals owing its antitumor efficacy is quite limited. Therefore, an intensive demonstration of cytotoxicity and identification of bioactive constituents of this partially explored plant (*E. milii*) is direly needed. In our search for chemopreventive agents from Asian flora, this study was undertaken to evaluate the antioxidant and anti-proliferative potential of the different fractions of methanol extracts of *E. milii* plant which is traditionally being used to treat hepatic disorders (Delgado et al., 2003). The present study, the chemopreventive potential of *E. milii* aerial parts has been systematically investigated using MTT assay, qRT-PCR and western blot analysis followed by GC–MS, molecular docking, molecular dynamic (MD) simulation and free energy calculation analysis. To the best of our knowledge, this is the first systematic report for the evaluation of chemopreventive potential, phytochemical profile and computational exploration of *E. milii* (aerial part); underling its significance as a source of bioactive chemotypes which have potential to be repurposed for cancer therapy.

2. Material and method

2.1. Materials

All solvents used for the extraction purpose were purchased from Merck (Germany). 5-Fluorouracil (5-FU) was purchased Sigma-Aldrich (St Louis, MO, USA). Antibodies against CDK2, cyclin E, and β-actin were purchased Santa Cruz Biotechnology (CA, USA) and E2F1 was purchased from Abcam (Cambridge, UK). All chemicals and reagents used in this study were of analytical grade.

2.2. Methods

2.2.1. Plant material collection and extraction

The plant material was collected from the surroundings of Tehsil Pattoki, District Kasur, Punjab province of Pakistan, during March, immediately few days after rain. The plant was identified as *Euphorbia milii* var. *(E. milii)* by Prof. Dr. Zaheer Ahmed from Department of Botany, Government College University, Lahore (GCUL), Pakistan. A specimen Voucher (voucher no. 2012) of the plant was submitted to Sultan Ayub Herbarium, GCUL. The collected plant material of *E. milii* was kept under a shade at room temperature for 15–20 days. The dried stems of *E. milii* were crushed to a coarse powder of approximately 60-mesh size using Willy Mill. For extraction, 2.5 Kg of weighed dried powder was macerated and extracted twice with 5 litter of methanol (MeOH) for five days. The obtained extracts were then concentrated to dryness at temperature 45 °C with rotary evaporator. 40 gm of crude MeOH extract of *E. milii* (Em-MeOH) was suspended in 800 mL of distilled water and successively partitioned using an equal volume of *n*-hexane, diethyl ether, chloroform, ethyl acetate and *n*-butanol to separate various phytochemicals on the basis of increasing solvent polarity. Finally, *n*-hexane, diethyl ether, chloroform, ethyl acetate, *n*-butanol and water fractions (Em-H, Em-D, Em-C, Em-EA, Em-B and Em-W, respectively) were dried using the aforementioned procedure and stored at room temperature till further analysis.

2.2.2. Free radical scavenging assay

The stable 1,1-diphenyl-2-picrylhydrazyl radical (DPPH) was utilized to investigate antioxidant potential (Koleva et al., 2002). Different concentrations of the compounds in their respective solvents were added at an equal volume (10 μL) to 90 μL of 100 μM of methanolic DPPH in a total volume of 100 μL in 96-well plates. The contents were mixed and incubated at 37 °C for 30 min. The absorbance was measured at 517 nm using a Synergy HT BioTek® USA microplate reader. Quercetin and L -ascorbic acid were used as standard antioxidants. The experiments were carried out in triplicate. IC_{50} values were calculated using the EZ-Fit5 (Perrella Scientific Inc., Amherst, USA) software. The decrease in absorbance indicated the increased radical scavenging activity, which was determined by the following formula as described previously.

$$\text{Percentage scavenging activity} = 100 - \left(\frac{\text{Abs of test fraction}}{\text{Abs of control}}\right) \times 100$$

2.3. Cytotoxicity assay

2.3.1. Cell culture and differentiation

The HeLa and HepG2 cells were gifted from cell bank of The University of Lahore (UOL), Lahore, Pakistan. Cells were cultured and maintained in Dulbecco’s modified Eagle’s medium (DMEM)

(Gibco, Carlsbad, CA) enriched with 10% FBS (Gibco) and 100 units/ml of penicillin–streptomycin in a 5% CO_2 humidified incubator at 37 °C.

2.3.2. In vitro cytotoxicity assay

To evaluate the effect of *E. milii* on tumor cell proliferation, HeLa and HepG2 cells were seeded in 96-well plates then allowed the cells to adhere overnight and treated with *E. milii* with following concentrations (1.87, 3.7, 7.4, 15, 30, 60, and 120 μg/ml) for 72 h. After incubation, 200 μL MTT solution in the concentration of 500μ g/ml was added to each well and kept on incubation for 4 h. All 6 fractions (Em-H, Em-D, Em-C, Em-EA, Em-B and Em-W) of Em-MeOH were separately dissolved in DMSO with concentrations (1.87, 3.7, 7.4, 15, 30, 60, and 120 μg/ml). After incubation, 100 μL of DMSO solution of each concentration dilution was placed into every well plate. MTT was reduced to form formazan within cancer cells. The reduction was qualitatively observed by the color change of MTT from yellow to blue. Finally, the absorbance was measured at 570 nm by the Multiskan Microplate Spectrophotometer (Thermo Scientific Wilmington, DE, US). Half-maximal inhibitory concentration (IC_{50}) values were calculated from the different concentrations. Standard used in this assay was 5-Florouacil (5-FU) in (1.87–120 μg/ml) concentration. Cell viability was calculated with the help of following formula as described previously (Mosmann, 1983).

$$\text{Percentage inhibition } (\%) = \frac{\text{O.D of treated cells}}{\text{O.D of positive}} \times 100$$

The results were generated from three independent experiments; each experiment was performed in triplicate. The IC_{50} values were calculated using CalcySyn™ (USA) software.

2.3.3. Quantitative RT-PCR assay

Total RNA from HepG2 cells were isolated using Easy Pure RNA Kit (Transgen Biotech Co., Ltd), and cDNA was synthesized. The sequences of the primers used for qRT-PCR are listed in Table S1 in the supporting information. qRT-PCR analysis was performed by BioRad SYBR Premix (Bio-Rad, Hercules, CA, USA). The reaction mixtures containing SYBR Green were prepared by following the manufacturer's protocol. Relative expression levels of the target genes were normalized with the control gene GAPDH.

2.3.4. Western blot analysis

Cells were seeded in 6-well plates at a density of $1x10^5$ cells per well for 24 h. After treatment with *E. milii* for the indicated time period, the cells were collected. Tumor cells were put in dry ice for 10 min in lysis buffer. The supernatants were collected after the centrifugation at 11,000 RPM for 20 min at 4 °C. The supernatant was collected and protein concentration was measured by Bradford assay. Equal amount of denatured protein samples was loaded on SDS-PAGE gels, then transferred onto nitrocellulose membrane. The nitrocellulose membranes were put into the blocking solution (5% fat free milk) for 1 h, then incubated the monoclonal anti-rabbit CDK2, cyclin E, E2F1 and anti-β-actin with shaking over night at 4 °C. The horseradish peroxidase (HRP)-conjugated secondary antibody given for at least 1 h, then chemiluminescence was detected using a chemiluminescence imaging system (Bio-Rad, Hercules, CA).

2.4. GC–MS analysis

Em-C fraction of Em-MeOH extract was subjected to GC–MS analysis using GCMS-QP2010 Ultra High-End GC–MS (Shimadzu Co., Japan) equipped with fused silica gel column (30 m length × 0.25 mm I. d. 0.25 μm film) and the detector with EI mode enabled at 70 electron volt (eV) of ionization energy. The phytochemical analysis was carried out by injecting 1 μL of the sample with a split ratio of 20:1. The inert Helium gas (99.9%) was used as carrier gas; while the flow rate was kept at 1 mL/min. The injector temperature was kept constant at 280 °C. At first, the GC-oven temperature was maintained at 50 °C (for 3 min), then ramped to 280 °C at the rate of 10 °C/min. The chromatograms were recorded using full scan mode and the compounds were identified by comparing the highly abundant peaks in obtained spectral data with the with molecular database library of GC–MS (Hossain et al., 2014).

2.5. Computational studies

2.5.1. Structure preparation and molecular docking

The top 3 highly abundant compounds i.e. benzodioxole derivative (BAN), cyclobarbital (CBT) and mephobarbital (MBT) identified by GC–MS analysis (Fig. S1 in the supporting information) were selected for molecular docking studies. 3D structures of selected compounds were constructed by Sybyl-X1.3/SKETCH module (Jain, 2003) followed by energy minimization according to the Tripos force field with Gasteigere Hückel atomic charge (Clark et al., 1989). All 3 ligands were post-processed with molecular dynamics (MD) approach to obtain bioactive geometrical conformation. The co-crystallized structure of CDK2, BCL2, caspase-3 (CASP3), topoisomerase II and thymidylate synthase (TS) were downloaded from RCSB Protein Data Bank (PDB ID: 2XMY (Wang et al., 2010); 2O2F (Bruncko et al., 2007), 3DEI (Du et al., 2008); 4FM9 (Wendorff et al., 2012) and 1JU6 (Sayre et al., 2001), respectively) to be regarded as starting points for molecular docking studies. In order to investigate the binding modes of compounds BAN, CBT and MBT in the active site of selected proteins, flexible molecular docking simulations were performed using Surflex-Dock module of molecular modeling software package *SYBYL-X 1.3* (Jain, 2003) by adopting the same protocol and parameters as reported in our previous publications (Chohan et al., 2016; Rehman et al., 2019). For each ligand-receptor complex system, at least 20 best docked poses were conclusively saved. The best putative poses of ligands were graded by adopting the Hammerhead scoring function. Surflex dock module employs an empirically derived consensus scoring (cScore) (Welch et al., 1996) function that combines Hammerhead's empirical scoring function (Jain, 2003, 1996), that is, D-score (dock score), G-score (gold score), Chem-Score, potential mean force (PMF) score and the total score with a molecular similarity method (morphological similarity) to generate and rank putative poses of ligand fragments. Similarly, the standard compound 5-fluorouracil (5-FU) was also docked into the TS using aforementioned protocol and parameters.

2.5.2. Molecular dynamics simulation studies

Keeping in view the findings of Western blot, qRT-PCR, and molecular docking analysis; the top ranked docking generated complexes i.e CDK2-BAN, CDK2-CBT, 5-FU-TS and CBT-TS were subjected to molecular dynamics (MD) simulations for 50 ns (ns). All MD simulations and molecular mechanics-based free energy calculations (MM/PB(GB)SA), were entirely carried out in AMBER16 software package (Gohlke and Case, 2004), following the same protocol and parameters as those described previously (Chohan et al., 2016; Rehman et al., 2019, 2020). Each of CDK2- and TS-bonded system was subjected to MD simulations at least for 50 ns using SANDER module in AMBER16 software package with the ff99SB force field (Duan et al., 2003). The ligands were energetically optimized by applying AM1 method (Becke, 1980) with HF/6- 31G* basis set in Gaussian 09 program. The force field parameters for the ligands were assigned using general AMBER force field (Berendsen et al., 1984) (GAFF) together with RESP

charges (Abu Sid, 1989). Missing hydrogens in receptors were added using LEaP program from AMBER 16. Each system was then immersed in an explicit TIP3P (Jorgensen et al., 1983) solvation model at 300 K temperature and 1 bar pressure. Cl^- and Na^+ counter-ions were added to neutralize CDK2- and TS-ligand complexes, respectively. Each system was relaxed by performing three consecutive steps of energy minimization and eight additional steps of MD equilibrations with gradually descending restraint weights (10 kcal·(mol·Å^2)$^{-1}$ to 0.1 kcal·(mol·Å^2)$^{-1}$) in a time of 100 ps per step at temperature 300 K. Finally, all four systems were subjected to MD simulation using NPT ensemble at aforementioned temperature and pressure (Ryckaert et al., 1977). The coordinates of MD simulation trajectories were collected at every 1 ps and 2 ps during equilibration and MD production run, respectively. All MD simulations procedures were carried out using the CARNAL, ANAL, and CPPTRAJ modules of AMBER16.

Free energy calculation. Molecular mechanics based scoring method MM/PB(GB)SA (Fogolari et al., 2003) of amber16 was utilized to compare the binding free energies of selected compounds in CDK2- and TS-bonded systems. The representative sets of equilibrium confirmations for the entire complex, individual receptor and free ligand were prepared and binding free energy was computed as a difference between the total free energy of ligand–protein complex (G_{com}) and sum of individual receptor (G_{rec}) and ligands (G_{lig}) free energy. At least 1000 snapshots for each complex, were taken from last the 5 ns stable MD trajectory at 5 ps intervals to predict the binding free energies (ΔG_{bind}).

2.6. Statistical analysis

Data were demonstrated as mean ± SD of at least triplicate experiments. The results were statistically analyzed by two-tailed unpaired Student's *t*-test. Differences were considered significant if the P value was less than 0.05.

3. Results and discussion

3.1. Extraction and fractionation

The extraction with methanol using cold maceration technique yielded a sufficiently good quantity of crude dry extract (78.32 g). The liquid–liquid extraction of the crude methanol extract (40.00 g) was carried out using solvents of increasing polarity (Fig. S2 in the supporting information) to separate the compounds according to their affinity towards the solvent used. Furthermore, Fig. S2 in the supporting information also depicts the extraction yield of dry fractions (Em-H, Em-D, Em-C, Em-EA, Em-B and Em-W). Em-B fraction showed the highest extraction yield (29.77%) followed by Em-W, Em-D and Em-C fractions which demonstrated relatively lower yields, i.e. 22.77%, 18.02% and 14.72%, respectively.

3.2. Free radical scavenging assay

In the human body, the overproduction of free radicals is directly associated with cell damage and ongoing biochemical reactions (Patel Rajesh and Patel, 2011). Various free radical-generating substances are included within our daily use-products such as food, medicines and the water. A plethora of studies has demonstrated that increased production of free radicals may induce various disorders, including cancer, myocardial infarction, atherosclerosis, and neurodegenerative disorders (Patel Rajesh and Patel, 2011; Uttara et al., 2009). Free radical scavengers (antioxidants) are compounds that may reduce the generation of free radicals to avoid oxidative stress related cell damages. To date, numerous antioxidant molecules have been identified in the plants of different origin and have demonstrated beneficial effects in treating various human ailments (Salganik, 2001). DPPH radical scavenging assay is one of the most frequently used approaches to determine the antioxidant potential of different plant extracts. This study aimed to evaluate the antioxidant and anti-proliferative properties of *E. milii*. As demonstrated in Fig. 1A, scavenging effect of different fractions of Em-MeOH extract on DPPH radical was in the following order Em-C > Em-EA > Em-D > Em-B > Em-H > Em-W fractions. Our results indicate that among all six fractions, the IC_{50} value for Em-C fraction (IC_{50}: 6.41 ± 0.99 μg/ml) was closest to that of the quercetin (IC_{50}: 1.69 ± 0.14 μg/ml). On the other hand, the Em-D and Em-EA fraction demonstrated only moderate antioxidant activity (IC_{50}: 9.12 and 7.48 ± 1.2 μg/ml, respectively) as compared to that of standard while the remaining fractions showed no significant antioxidant activity. Taking together, the aerial part of *E. milii* possess good to moderate antioxidant activity and the scavenging activity of the different fractions increases in a concentration-dependent manner (Fig. 1B).

3.2.1. In vitro cytotoxicity assay

Plants are a promising source of anti-infective and anticancer chemotherapeutic agents. In the present study, cytotoxicity assay was studied on HeLa and HepG2 cell lines and evaluated by MTT method. All 6 fractions of Em-MeOH extract (Fig. S2 in the supporting information) were screened for *in vitro* anticancer activity against human HeLa and HepG2 cancer cell lines. 5-FU was used as a positive control. Each extract was screened initially for its cytotoxicity against cancerous cells at the eight different concentrations starting from 1.8 μg/ml up to 120 μg/ml. The potential candidates which resulted in cell survival of less than 50% were further assessed for their IC_{50}.values at concentration range 1.87–120 μg/ml. The IC 50 values were calculated using CalcySyn™ (USA) software. In case of HeLa cell line, MTT assay was performed on MeOH extract and its 6 fractions in the solvents of increasing order of polarity, and then IC_{50} was calculated. The Em-C was identified as more potential fraction with superior inhibition potential (59.61%) against HeLa cell line than Em-MeOH extract (52.59%). However, the cytotoxic potential of Em-C remained inferior in HeLA cell line to that of standard compound 5-FU (88.38%).

Likewise, the anti-cancer potential of Em-MeOH extract and its 6 fractions were investigated by MTT assay on HepG2 cell line. Em-MeOH displayed appreciable cytotoxicity against HepG2 cells by inducing 62.54% inhibition of invasive cell growth. The potential fractions of Em-C demonstrated the most significant cytotoxic potential (76.61%) among all tested fractions against HepG2 cell line. Although, the 5-FU has demonstrated superior cytotoxic potential (92.29%) than Em-C (76.61%) against HepG2 cell; the cytotoxic potential of Em-C was found to be significant as no considerable difference in growth inhibition was observed. Conversely, Em-EA showed moderate inhibition potential (63.80%) when compared to the Em-C and slandered 5-FU (73%). Apart from, Em-C and Em-EA, other fractions did not show considerable cytotoxic potential at any dose. Furthermore, the detailed description antiproliferative activity of the tested fractions and 5-FU as determined by the MTT-assay are summarized in Table 1. The findings of cytotoxicity analysis suggest that the Em-C fraction has significant anti-proliferative effects against HepG2 than HeLa cells.

3.2.2. E. milii extract downregulates the expressions of cell cycle regulators in vitro

CDK2-E2F1 pathway is critical in regulating the transition of G1 to S phase of the cell cycle. CDK2 is one of the members of cyclin-dependent kinases (CDKs) (Chen et al., 2012; Tin et al., 2012). Since Em-C has demonstrated the highest cytotoxic potential against HepG2 cell lines. In the present study, gene expression analysis was performed to reveal the variation in gene expression upon pro-

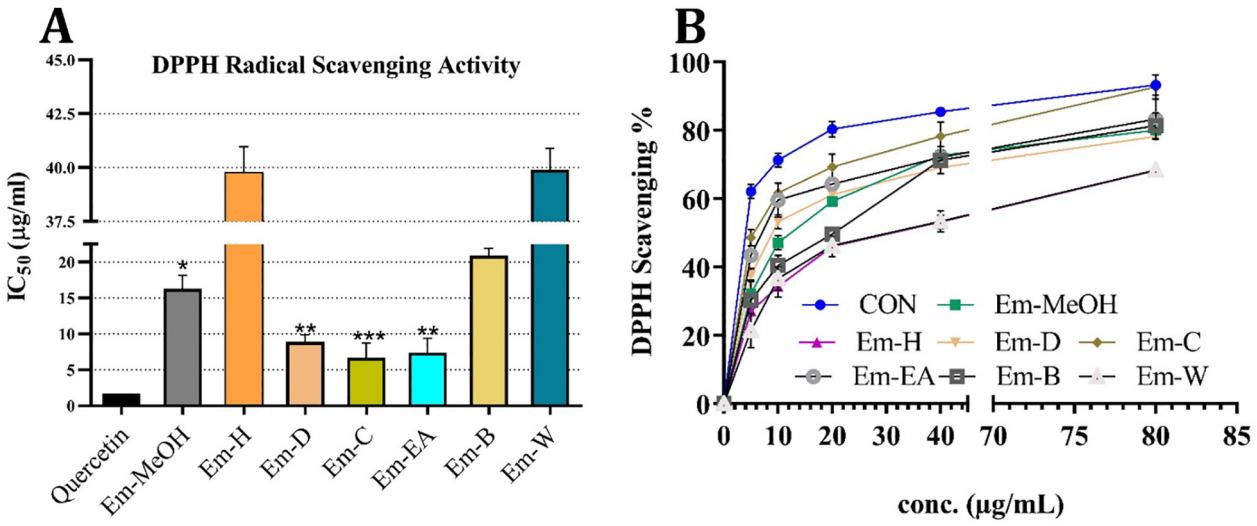

Fig. 1. DPPH free radical scavenging activities of selected extracts. (A) Half-maximal concentration (IC_{50}) of various solvent fractions from methanol extract of *E. milii*. (B) Dose dependent DPPH scavenging activity.

Table 1
Cytotoxicity evaluation of extract (Em-MeOH), its fractions and 5-fluorouracil towards cancer cell lines (Hela and HepG2.) as determined by the MTT-assay.

	Hela cells		HepG2	
Sample code	% Inhibition/Stimulation	IC_{50} ± SD	% Inhibition/Stimulation	IC_{50} ± SD
Em-MeOH	52.59	27.9 ± 0.2	62.54	15.9 ± 0.3
Em-H	inactive	–	inactive	–
Em-D	inactive	–	inactive	–
Em-C	59.61	22.1 ± 0.8	76.61	11.2 ± 0.8
Em-EA	inactive	–	63.80	20.4 ± 0.4
Em-B	inactive	–	inactive	–
Em-W	inactive	–	inactive	–
5-FU	88.38	6.87 ± 0.5	92.29	4.22 ± 0.6

Em-H, Em-D, Em-H, Em-EA, Em-B and Em-W are fractions of MeOH extract in six solvents in the increasing order of polarity like n-hexane, diethyl ether, chloroform, ethyl acetate, n-butanol and water respectively. Em-MeOH = Methanolic extract of the stem of *Euphorbia milii*. 5-Fu = 5-Fluorouracil. IC_{50} = the concentration of compound that inhibits 50% of cell growth.

longed exposure to IC_{50}-dose of Em-C. Gene expression analysis of HepG2 cells upon exposure to various treatments has previously been reported (Chen et al., 2012); suggesting that the disruption of CDK2-E2F1 pathway either by CDK2 or E2F1 inhibition may lead to the suppression of invasive growth of HepG2 cells. Keeping in view the previous reports (Chen et al., 2012), the variation in the expression of cell cycle regulatory genes i.e. CDK2, cyclin E and E2F1 in HepG2 cells exposed to IC_{50}-dose Em-C fraction for 24 h. During gene expression analysis, Em-C at IC_{50} dose displayed 5-fold downregulation in CDK2 gene expression (Fig. 2A). Whereas, only 2-fold downregulation in the expression of E2F1 gene was observed. Conversely, no reduction in the expression of cyclin E was observed (Fig. 2A). These results suggest that the significant cytotoxicity of Em-C was the consequence of G0/G1 phase arrest, generally by hampering the expression of CDK2, which ultimately suppresses the HepG2 cell division through the CDK2-E2F1 pathway *in vitro*.

Furthermore, we sought out to investigate the molecular mechanisms by investigating the cell cycle-related proteins. The effect of Em-C on the expression of CDK2, E2F1 and cyclin E has been investigated *in vitro* using western blot analysis. The HepG2 cells were treated with Em-C for 24 h. The results indicated that Em-C fraction of EM-MeOH markedly downregulated the expression levels of CDK2 and E2F1 with no significant effects on cyclin E (Fig. 2B). Since, Em-C caused a significant decrease in the expression of mRNA levels of CDK2 and E2F1, it indicates that *E. milii* has a potential to inhibit CDK2-E2F1 pathway.

Accumulated evidences supported the fact that the growth of cancer cells could be inhibited via downregulation of mRNA or protein levels of CDK2, cyclin E or E2F1 transcription factor. Tin *et al* (Matsuda, 2008) reported that artemisinin inhibited the proliferation of breast cancer cells via selectively downregulating the levels of the CDK2 and CDK4, cyclin E, cyclin D1 and the E2F1 transcription factor. Fang et al. (2011) reported that acetylbritannilactone inhibited the growth of HT-29 human colon cancer cells by inducing cell cycle arrest in G0/G1 phase and this suppression was accompanied by a marked decrease of cyclin E and CDK4 protein levels. In present study, we propose that the cytotoxic effect of *E. milii* on invasive growth of HepG2 cells were associated with protein levels of CDK2 and E2F1 involved in CDK2/Rb/E2F signaling. Our results showed that *E. milii* interfered and downregulated the transcription of protein levels of CDK2 and E2F1 transcription factor. Further phytochemical investigation to reveal chemotypes responsible for downregulation in CDK2 expression may help to identify novel CDK2 inhibitor.

3.2.3. GC–MS analysis of Em-C fraction

GC–MS evaluation of Em-C fraction of Em-MeOH extract was performed to identify the phytochemical constituents that are responsible for antioxidant and anti-proliferative properties of Em-C fraction. Fig. 3 represents the distinct chromatogram of Em-C fraction from Em-MeOH extract. The list of identified compounds along with their peak number, retention time (RT), and peak area (%) are tabulated in Table S4 in the supporting informa-

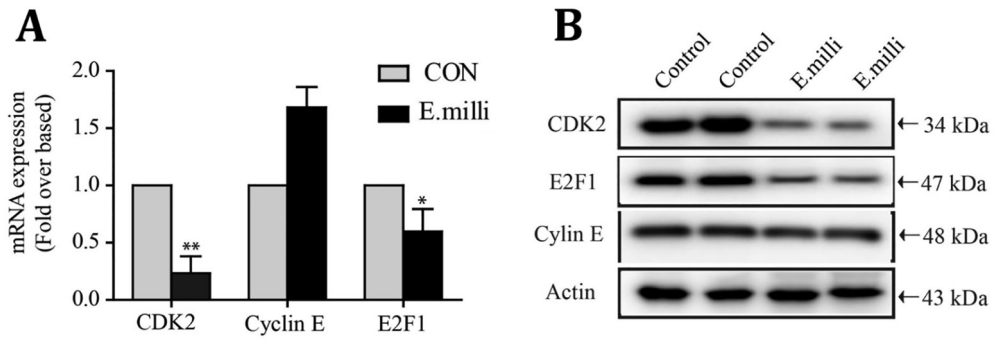

Fig. 2. Effect of *E. milii* on mRNA expression of specific gene of cell cycle regulators. (A) qRT-PCR was performed to assess the mRNA levels of cells regulators genes. HepG2 cells were cultured in the presence or absence of 11.2 μM *E. milii* water extract for 24 h. The GAPDH was used as internal positive control. The data for *E. milii*-treated samples were presented as the mean ± SEM of triplicate determination and compared with the control group. $^{*}p < 0.05$; $^{**}p < 0.01$. (B) Effect of *E. milii* on expression of cell cycle regulators. The cells were treated with or without *E. milii* for indicated time. The expression of CDK2, E2F1 and cyclin E were determined with western blot analysis.

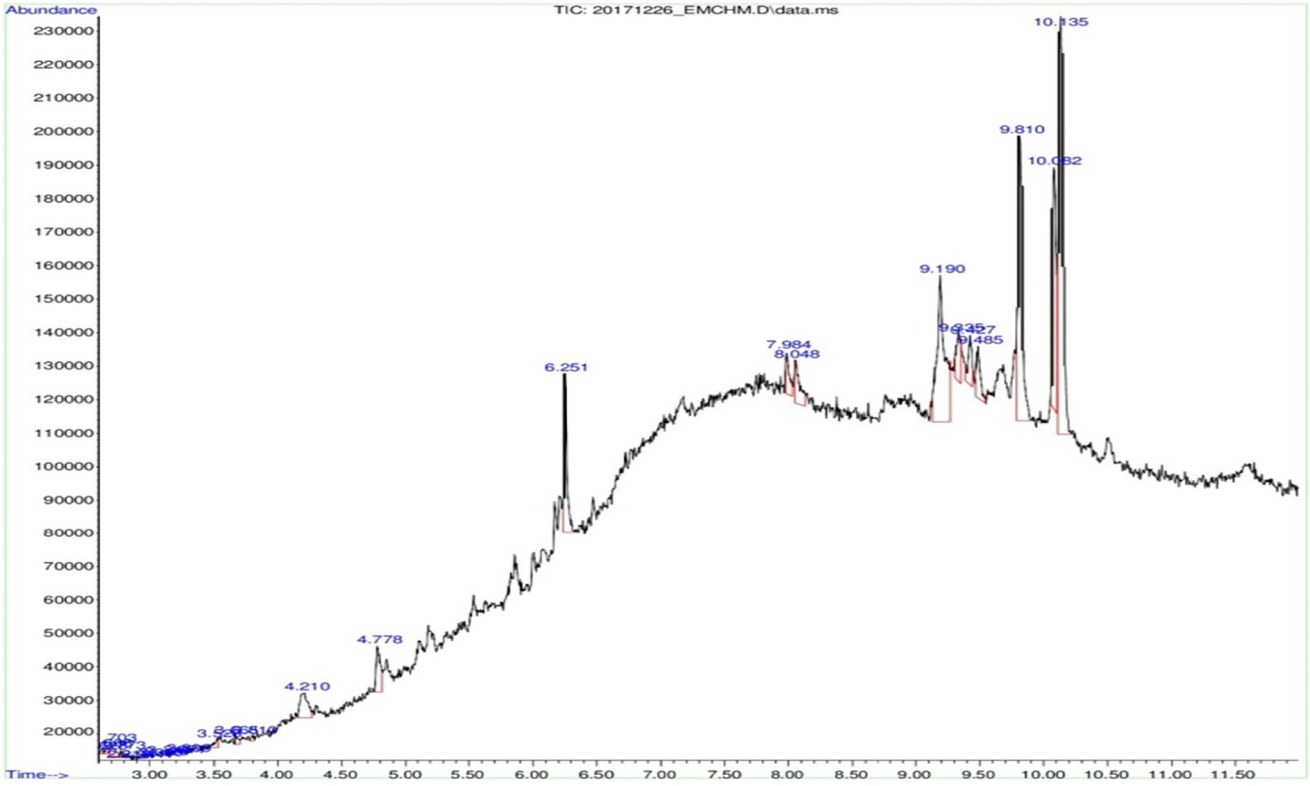

Fig. 3. GC–MS chromatogram for identification of compounds in Em-C.

tion. Out of 25 peaks observed in the chromatogram of Em-C fraction, 10 compounds were identified with major peaks. The most abundant compounds included mephobarbital (36.11%), N-methyl-N-acetyl-3,4-methylenedioxybenzylamine (24.03%) and cyclobarbital (18.15%). Although, the literature survey reveals the occurrence of N-methyl-N-acetyl-3,4-methylenedioxybenzylamine (BAN) (Jamuna and Paulsamy, 2013) and cyclobarbital (CBT) from various plant sources (Maitra et al., 2019; Charoensiddhi and Anprung, 2008; Ashraf et al., 2015); there is no report of GC–MS based metabolite profiling to detect the unique presence of benzodioxole and barbital derivatives from any part of *E. milii* and we are the first time to report the occurrence of these compounds (BAN and CBT) in aerial part of *E. milii*. Although, the cyclobarbital being a barbiturate, is a well-known anticonvulsant and hypnotic agent; recently it has also been reported to poses anti-proliferative potential (Maitra et al., 2019). In addition, some other bioactive compounds identified by GC–MS include palmitic acid, butanoic acid, 3-amino-1-phenylbutane acetyl derivative and stearic acid (Table S3 in the supporting information). Conclusively, the substantial antioxidant and anti-proliferative activities of Em-C fraction could be correlated with the occurrence of these bioactive compounds. In particular, the significant anti-proliferative potential of Em-C fraction in biological evaluation might be attributed to the occurrence of major chemotypes i.e. BAN, CBT and MBT. Since the anticancer potential of these compounds has not been critically investigated; an intensive research on repurposing of BAN, CBT, and MBT as anticancer agent is direly needed.

3.2.4. In-silico studies

In-silico approach may provide substantial knowledge of structural and functional relationship in ligand–protein systems to understand the molecular mechanism for variations in target gene

expression and their corresponding proteins. During gene expression and western blot analysis (Fig. 2A and B, respectively), the expression of CDK2 protein was observed to be significantly down-regulated upon continuous exposure to Em-C fraction. Meanwhile, the GC–MS analysis of Em-C has revealed the presence of BAN, CBT and MBT (Fig. S1 in the supporting information) as major components. Therefore, molecular docking with subsequent MD simulations has been performed to identify the potential chemotype responsible for anti-proliferative potential of *E. milii* through CDK2 inhibition. Furthermore, to compare the binding mode of selected compounds with standard one; the compounds BAN, CBT, and MBT along with standard compound 5-FU has been docked into the active site of thymidylate synthase (TS). In addition, a comprehensive literature survey was performed to identify three more proteins BCL2, CASP3 and topoisomerase II regulating distinct signaling pathways in HepG2 cells for molecular docking studies. The findings of computational studies are in strongly correlated to the experimental results and provide a reasonable explanation regarding the significant chemopreventive ability of Em-C fraction against HepG2 cell lines.

3.2.5. Molecular docking and MD simulation

In present work, 3 major compounds (BAN, CBT, and MBT) from Em-C fraction of *E. milii* were docked in to the active site of various molecular targets i.e. CDK2, BCL2, CASP3, topoisomerase II and TS using Surflex-Dock module of SYBYL-X 1.3. (Jain, 2015). The docking scores (*Cscore*) of BAN, CBT and MBT for CDK2 are 5.03, 4.18 and 3.55 respectively, which indicates that BAN exhibit substantial binding affinities towards CDK2. However, CBB and CBT displayed moderate to weak binding affinity towards CDK2 (*Cscore* = 4.18 and 3.55, respectively). Moreover, the docking comparison with standard compound has revealed that 5-FU and CBB exhibit higher binding affinity towards TS (*Cscore* = 5.01 and 4.81, respectively) than CBT-TS complex (*Cscore* = 3.14). Conversely, all three compounds have displayed moderate to weaker binding affinity towards BCL2, CASP3 and topoisomerase II proteins. The corresponding docking scores and key residues involved in H-bonding are summarized in Table S3 of supplementary information. Moreover, the docking conformations of studied ligands bonded to BCL2, CASP3 and topoisomerase II are depicted in Fig. S3 of supplementary information.

To inspect the molecular features responsible for variations in binding affinity of selected ligands towards CDK2; the top-ranked docking conformations for all three ligands in their respective complexes were saved. Fig. S4 in the supplementary information represents simplified 2D-interaction diagrams to explore variations in ligand–protein interaction pattern. Docking results show that all ligands acquire similar mode of interaction within the active site of CDK2 where Lys33, Glu81, Phe82 Leu83, and Asp145 are the key residues constituting the ligand binding site in CDK2. In CDK2-BAN complex (Fig. 4A–C), although BAN establish a single H-bond interaction with hinge residue Leu83, the superior binding affinity of BAN in CDK2-BAN system is mainly attributed by additional H-bond interaction with Lys33 and the possible van der waals (*vdW*) contacts between methyl group of BAN and negatively charged oxygen in Asp145 of CDK2. The methyl group at tertiary

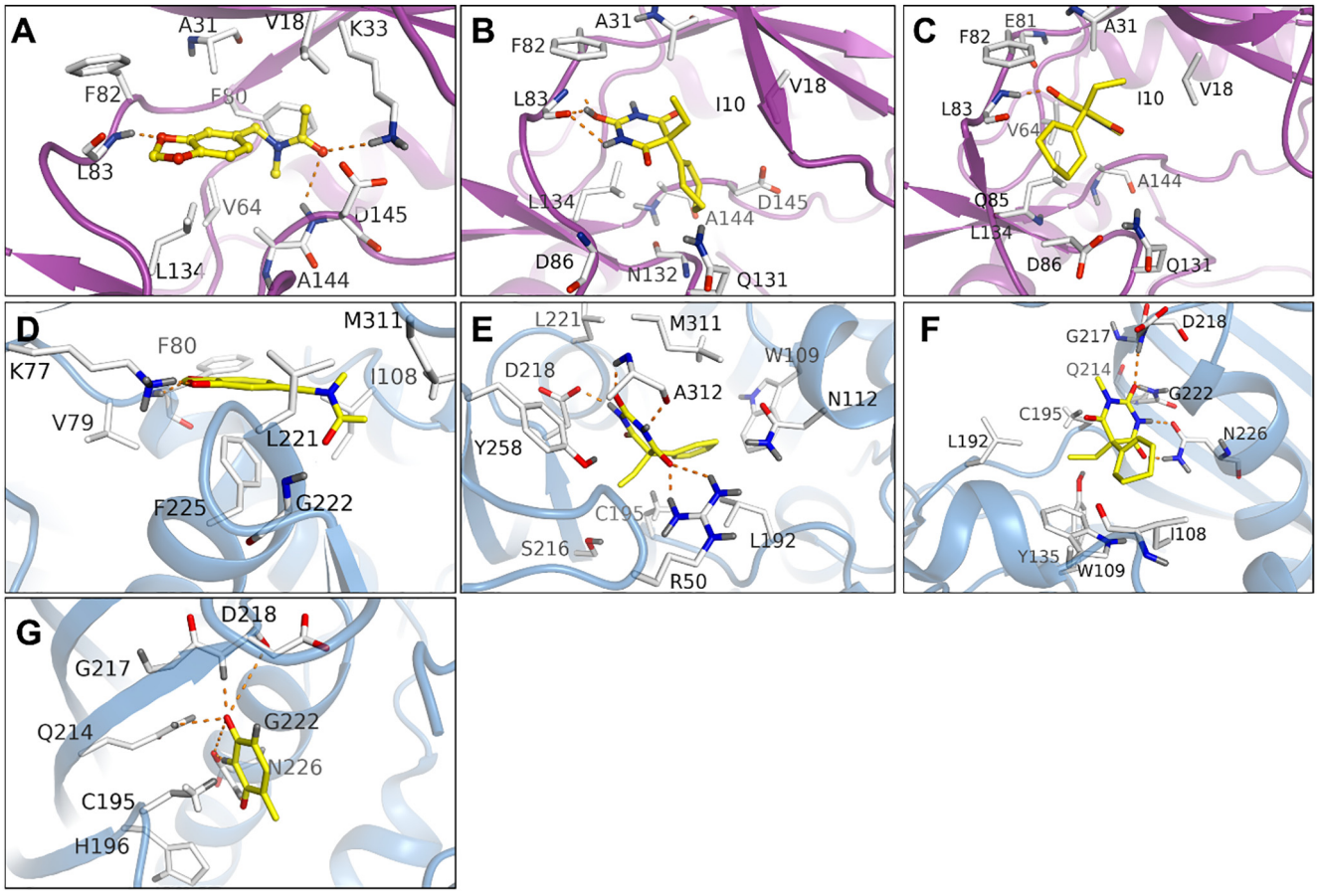

Fig. 4. Obtained binding modes of ligands in the binding domain of CDK2 (magenta) and Thymidlate synthase (skyblue). (A) Binding mode of compound BAN in CDK2 ATP binding site. (B) Compound CBT bonded to CDK2. (C) Docking complex of CDK2-MBT. Binding mode of selected compounds in the active site of Thymidlate synthase (TS): (D) BAN-TS, (E) CBT-TS, (F) MBT-TS and (G) compound 5-FU (standard) bonded to TS.

amine of BAN is extended towards a so-called phenyl-80 pocket to establish hydrophobic contacts with surrounding residues. Although, CBT also establishes conserved pattern of H-bond interactions with Glu81 and Leu83 in hinge region of CDK2 as that observed in CDK2-BAN and many other CDK2-inhibitor complexes; unlike CDK2-BAN complex CBT lacks H-bond with Lys33 which may attribute to its moderate binding affinity towards CDK2. Interestingly, Lys33, Asp86, Gln131, Ala141 and Asp145 are crucial for catalytic activity of CDK2 and it's binding to substrate. The substantial role of these residues in ligand binding selectivity has already been extensively discussed previously (Chohan et al., 2016), which supports the accuracy of our docking results. Apart from the fact that MBT exhibit almost same structure as that of CBT; the compound MBT fails to establish conserved H-bond interactions in hinge region of CDK2 due to replacement of amino hydrogen of CBT with a methyl substituent in MBT (Fig. 4C and Fig. S4 of supplementary information). This minor variation in structure of MBT leads to an unstable orientation of MBT in its corresponding complex which may explain decreased binding affinity MBT towards CDK2.

As depicted in Fig. 4D-G, the standard compound 5-FU successfully establishes a set of five hydrogen bonds (H-bond) with residue Gln214, Gly217, Asp218, Asn226 in a donor–acceptor-donor motif. Furthermore, the fluoro-group at 5th position of uracil moiety is headed towards a shallow hydrophobic sub-site of TS constituted by residues Trp199 and Cys195 to establish various hydrophobic contacts (Fig. 4G). Unlike 5-FU, benzodioxole moiety in BAN establishes only a couple of H-bond interaction in TS binding site, which may explain decreased binding affinity of BAN toward TS (Fig. 4D). As shown in Fig. S4 in the supporting information, CBT share high structural similarity with that of 5-FU. In CBT 5-fluoro group of 5-FU is replaced by a cyclohexene moiety and ethyl chain. Docking results show that CBT establishes at least five H-bond interactions with residues Arg50, Thr51, Gln214, Asp218 and Ala312. Moreover, the C-5 cyclohexyl and ethyl moieties are settled in a cavity constituted by residues Trp109, Cys195, Leu192 and Ser216 to establish several hydrophobic and *vdW* contacts with nearby residues. Hence, these additional interactions mainly attribute to the similar binding affinity of CBT towards TS as that observed in TS-5-FU system. MBT establishes conserved H-bond interactions with Gln214 and Asp218. However, no interaction with residues Arg50, Thr51 and Ala312 was observed which may explain decreased binding affinity of MBT for TS than MBT. In short, the findings of docking studies suggest that the compounds BAN and CBT are the key components in Em-C fraction might be responsible for its substantial cytotoxic activity against HepG2 cells by synergistically inhibiting CDK2 and TS, respectively.

3.2.6. MD simulation, MM/PB(GB)SA

In order to study dynamic stability of selected docked structures, top four docking complexes (CDK2-BAN, CDK2-CBT, 5-FU-TS and CBT-TS) were post-processed with MD simulations to investigate the key molecular interactions responsible for ligand-receptor binding under physiological conditions. All four complexes were subjected to 50 ns MD simulations and stability of studied complexes was elucidated by computing RMSD. As

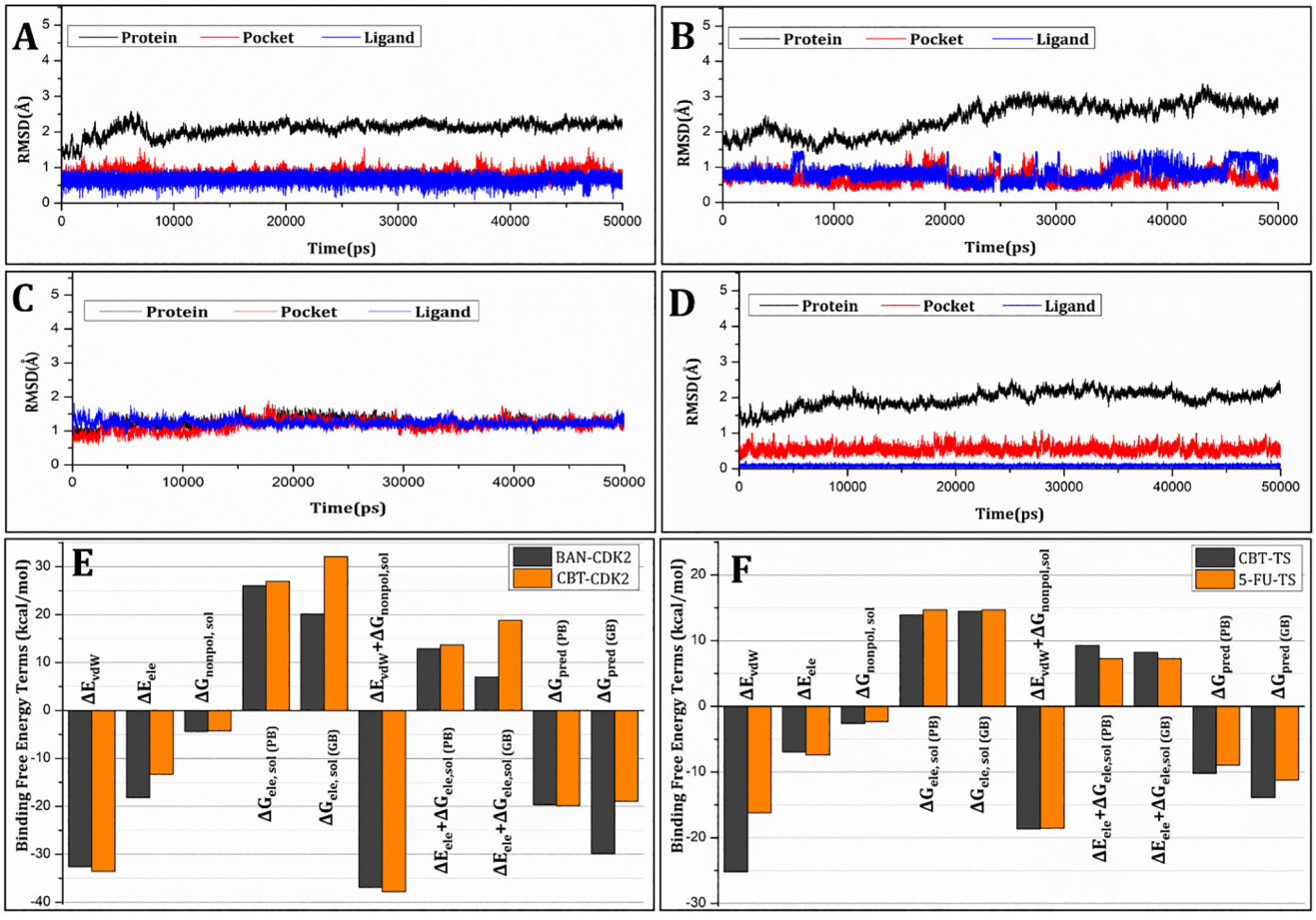

Fig. 5. RMSDs of Cα atoms of the protein, backbone atoms of binding pocket (within 6.5 Å), and the heavy atoms in the ligand for: (A) CDK2-BAN, (B) CDK2-CBT, (C) TS-CBT and (D) TS-5-FU. Comparison between binding free energy terms of: (E) CDK2 bonded to BAN and CBT; (F) TS bonded to CBT and 5-FU.

illustrated in Fig. 5A–D, all complex systems remained stable throughout the simulation period and RMSD remained below 2.5 Å for protein, pocket or ligand. Among all 4 complexes, 5-Fu displayed lowest RMSD value due to its smaller structure (Fig. 5D). Furthermore, the comparison of MD-simulated averaged coordinates of CDK2-ligand complexes super-positioned on their respective starting complexes (Fig. S5 of supplementary information) has revealed that all ligand remained firmly bonded to their corresponding complexes with no loss of key interactions. Hence, the ligand–protein complex stabilization analysis suggests that docking simulated conformations are correct enough to be used for computing binding free energies.

Last but not least, an exhaustive analysis of the computed binding affinities of BAN and CBT towards CDK2 has been performed by employing MM/PB(GB)SA approach. The binding free energy values $\Delta G_{pred\ (GB)}$ computed by MM/PB(GB)SA approach reveals that both compound BAN (-29.85 kcal·mol^{-1}) is more strongly bonded to CDK2 than the CBT (-18.92 kcal·mol^{-1}, respectively). Since, BAN showed the most significant difference in $\Delta G_{pred\ (GB)}$ values for CDK2 in contrast to CBT; it reflects that the compound BAN is the most selective CDK2 inhibitor among all three inhibitors. Likewise, the MM/PBSA computed free energies ($\Delta G_{pred\ (PB)}$) also depict the ranking of binding affinities; which, indicates that BAN interacts more efficiently with CDK2 ($\Delta G_{pre(PB)}$ -19.68 kcal•mol^{-1}; -16.84 kcal•mol^{-1}, respectively) than CBT. The cumulative MM/PB(GB)SA binding free energies were decomposed into independent energy components to reveal deriving forces responsible for difference in binding affinities of studied ligands towards CDK2. Fig. 5E demonstrate a comparison of individual energy components for BAN and CBT bonded systems. As shown in Fig. 5E, the *vdW* and the nonpolar solvation energy (ΔE_{vdW} + $\Delta G_{nonpol,sol}$) contributions arising either from σ–π stacking, *vdW* contacts and/or the burial of the hydrophobic moieties are almost same for BAN and CBT (-36.87 kcal·mol^{-1}; -37.86 kcal·mol^{-1}, respectively. Despite of similar ΔE_{vdW} + $\Delta G_{nonpol,sol}$ and ΔG_{ele} contribution, the smaller $\Delta G_{pred(GB)}$ values for CBT system than BAN system are the consequence of lower unfavorable polar solvation ($\Delta G_{ele+pol}$) energies (Fig. 5E) and favorable ΔG_{ele} values in BAN bonded system than CBT-CDK2 complexes. Conclusively, the *vdW* and electrostatic interactions have been identified as key components responsible for improved binding affinities of BAN and CBT for CDK2. Furthermore, binding free energy was also computed for CBT-TS complex to compare with 5-FU-TS system (Fig. 5F). The computed $\Delta G_{pred\ (GB)}$ value show that CBT (-13.88 kcal·mol^{-1}) is more strongly bonded to TS than the standard compound 5-FU (-11.25 kcal·mol^{-1} kcal·mol^{-1}, respectively). As depicted in Fig. 5F, the major contribution to the difference in binding free energies of CBT- and 5-FU-TS was primarily made by different *vdW* and nonpolar solvation energies. Thus, on the basis of experimental and computational findings; we may propose that compounds BAN and CBT remarkably potentiated the anticancer effect of EmC by simultaneously downregulating the protein level of CDK2 and thymidylate synthase.

4. Conclusions

The findings of the present study identify *E. milii* as a novel source of barbital and benzodioxole derivatives. The unique occurrence of cyclobarbital and benzodioxole derivative as major components in Em-C fraction of Em-MeOH extract as predicted by GC–MS analysis may have contributed the remarkable potential of Em-C fraction to suppress the invasive growth of HepG2 cancer cells. Results of gene expression profiling and western blot analysis have identified the maximum downregulation in the expression of CDK2 protein while moderate variations in the expression of E2F1 proteins have also been observed. However, no noticeable effect was observed on cyclin-E expression. *In-silico* studies further reinforce the fact that the primary components BAN and CBT forms relatively stronger and stable complexes with CDK2 and thymidylate synthase, respectively. Molecular docking structures of inhibitors (5-FU, BAN and CBT) bound to TS revealed that the binding mode of selected inhibitors is conserved. In CDK2 bonded system CBT form more stable complexes than CDK2-CBT system by exploiting additional interactions in catalytic and Phenyl-80 subsite of ATP-binding pocket, resulting in effective inhibition of CDK2. Conclusively, our results propose that the major components in *E. milii* can effectively inhibit the invasive growth of HepG2 cells by simultaneous inhibition of CDK2 and TS expression.

Declaration of Competing Interest

The authors declare that they have no known competing financial interests or personal relationships that could have appeared to influence the work reported in this paper.

Acknowledgements

The authors extend their appreciation to The University of Lahore (UOL), Lahore, Pakistan and Pakistan Council of Scientific Industrial Research (PCSIR), Lahore, Pakistan, for providing facilities to perform biological and phytochemical analysis, respectively.

Appendix A. Supplementary material

Supplementary data to this article can be found online at https://doi.org/10.1016/j.sjbs.2020.08.003.

References

Ashraf, A., Sarfraz, R.A., Anwar, F., Shahid, S.A., Alkharfy, K.M., 2015. Chemical composition and biological activities of leaves of Ziziphus mauritiana L. native to Pakistan. Pak. J. Bot. 47 (1), 367–376.

Bani, S., Kaul, A., Khan, B., Gupta, V.K., Satti, N.K., Suri, K.A., et al., 2007. Anti-arthritic activity of a biopolymeric fraction from *Euphorbia tirucalli*. J. Ethnopharmacol. 110 (1), 92–98.

Becke, A.D., 1980. Density thermochemistry. I. The role of exact exchange. J. Chem. 98 (7), 5648–5660.

Berendsen, H.J., Jv, Postma, van Gunsteren, W.F., DiNola, A., Haak, J., 1984. Molecular dynamics with coupling to an external bath. J. Chem. Phys. 81 (8), 3684–3690.

Bray, Freddie, Ferlay, Jacques, Soerjomataram, Isabelle, Siegel, Rebecca L., Torre, Lindsey A., Jemal, Ahmedin, 2018. Global cancer statistics 2018: GLOBOCAN estimates of incidence and mortality worldwide for 36 cancers in 185 countries. CA Cancer J. Clin. 68 (6), 394–424. https://doi.org/10.3322/caac.v68.610.3322/caac.21492.

Bruncko, M., Oost, T.K., Belli, B.A., Ding, H., Joseph, M.K., Kunzer, A., et al., 2007. Studies leading to potent, dual inhibitors of Bcl-2 and Bcl-xL. J. Med. Chem. 50 (4), 641–662.

Chaman, S., Khan, F.Z., Khokhar, R., Maab, H., Qamar, S., Zahid, S., et al., 2019. Cytotoxic and antiviral potentials of Euphorbia milii var. splendens leaf against Peste des petits ruminant virus. Trop. J. Pharm. Res. 18 (7), 1507–1511.

Charoensiddhi, S., Anprung, P., 2008. Bioactive compounds and volatile compounds of Thai bael fruit (Aegle marmelos (L.) Correa) as a valuable source for functional food ingredients. Int. Food Res. J. 15 (3), 287–295.

Chen, X.-Z., Cao, Z.-Y., Chen, T.-S., Zhang, Y.-Q., Liu, Z.-Z., Su, Y.-T., et al., 2012. Water extract of Hedyotis Diffusa Willd suppresses proliferation of human HepG2 cells and potentiates the anticancer efficacy of low-dose 5-fluorouracil by inhibiting the CDK2-E2F1 pathway. Oncol. Rep. 28 (2), 742–748.

Chohan, T.A., Qian, H., Pan, Y., Chen, J.-Z., 2015. Cyclin-dependent kinase-2 as a target for cancer therapy: progress in the development of CDK2 inhibitors as anti-cancer agents. Curr. Med. Chem. 22 (2), 237–263.

Chohan, T.A., Chen, J.-J., Qian, H.-Y., Pan, Y.-L., Chen, J.-Z., 2016. Molecular modeling studies to characterize N-phenylpyrimidin-2-amine selectivity for CDK2 and CDK4 through 3D-QSAR and molecular dynamics simulations. Mol. BioSyst. 12 (4), 1250–1268.

Chohan, T.A., Qayyum, A., Rehman, K., Tariq, M., Akash, M.S.H., 2018. An insight into the emerging role of cyclin-dependent kinase inhibitors as potential therapeutic agents for the treatment of advanced cancers. Biomed. Pharmacother. 107, 1326–1341.

Clark, M., Cramer III, R.D., Van Opdenbosch, N., 1989. Validation of the general purpose Tripos 5.2 force field. J. Comput. Chem. 10 (8), 982–1012.

Delgado, I., De-Carvalho, R., De-Oliveira, A., Kuriyama, S., Oliveira-Filho, E., Souza, C., et al., 2003. Absence of tumor promoting activity of *Euphorbia milii* latex on the mouse back skin. Toxicol. Lett. 145 (2), 175–180.

Du, J.-Q., Wu, J., Zhang, H.-J., Zhang, Y.-H., Qiu, B.-Y., Wu, F., et al., 2008. Isoquinoline-1, 3, 4-trione derivatives inactivate caspase-3 by generation of reactive oxygen species. J. Biol. Chem. 283 (44), 30205–30215.

Duan, Y., Wu, C., Chowdhury, S., Lee, M.C., Xiong, G., Zhang, W., et al., 2003. A point-charge force field for molecular mechanics simulations of proteins based on condensed-phase quantum mechanical calculations. J. Comput. Chem. 24 (16), 1999–2012.

Fang, X.-M., Liu, B., Liu, Y.-B., Wang, J.-J., Wen, J.-K., Li, B.-H., et al., 2011. Acetylbritannilactone suppresses growth via upregulation of krüppel-like transcription factor 4 expression in HT-29 colorectal cancer cells. Oncol. Rep. 26 (5), 1181–1187.

Fogolari, F., Brigo, A., Molinari, H., 2003. Protocol for MM/PBSA molecular dynamics simulations of proteins. Biophys. J. 85 (1), 159–166.

Gohlke, H., Case, D.A., 2004. Converging free energy estimates: MM-PB (GB) SA studies on the protein–protein complex Ras-Raf. J. Comput. Chem. 25 (2), 238–250.

Hossain, M.A., Al-Hdhrami, S.S., Weli, A.M., Al-Riyami, Q., Al-Sabahi, J.N., 2014. Isolation, fractionation and identification of chemical constituents from the leaves crude extracts of Mentha piperita L grown in Sultanate of Oman. Asian Pacific J. Trop. Biomed. 4, S368–S372.

Jain, A.N., 1996. Scoring noncovalent protein-ligand interactions: a continuous differentiable function tuned to compute binding affinities. J. Comput. Aided Mol. Des. 10 (5), 427–440.

Jain, A.N., 2003. Surflex: fully automatic flexible molecular docking using a molecular similarity-based search engine. J. Med. Chem. 46 (4), 499–511.

Jamuna, S., Paulsamy, S., 2013. GC-MS analysis for bioactive compounds in the methanolic leaf and root extracts of Hypochaeris radicata L. (Asteraceae). Int. J. Curr. Res. 5 (12), 4070–4074.

Jorgensen, W.L., Chandrasekhar, J., Madura, J.D., Impey, R.W., Klein, M.L., 1983. Comparison of simple potential functions for simulating liquid water. J. Chem. Phys. 79 (2), 926–935.

Kaur, R., Kapoor, K., Kaur, H., 2011. Plants as a source of anticancer agents. J. Nat. Prod. Plant Resour. 1 (1), 119–124.

Koleva, I.I., Van Beek, T.A., Linssen, J.P., Groot, Ad., Evstatieva, L.N., 2002. Screening of plant extracts for antioxidant activity: a comparative study on three testing methods. Phytochem. Anal.: Int. J. Plant Chem. Biochem. Techn. 13 (1), 8–17.

Kumar, A., Patil, D., Rajamohanan, P.R., Ahmad, A., 2013. Isolation, purification and characterization of vinblastine and vincristine from endophytic fungus Fusarium oxysporum isolated from Catharanthus roseus. PLoS ONE 8, (9) e71805.

Maitra, S., De, A., Das, B., Roy, S.N., Chakraborty, R., Samanta, A., et al., 2019. Seasonal variation of phyto-constituents of tea leaves affects antiproliferative potential. J. Am. Coll. Nutr. 1–9.

Matsuda, Y., 2008. Molecular mechanism underlying the functional loss of cyclindependent kinase inhibitors p16 and p27 in hepatocellular carcinoma. World J. Gastroenterol.: WJG. 14 (11), 1734.

Mosmann, T., 1983. Rapid colorimetric assay for cellular growth and survival: application to proliferation and cytotoxicity assays. J. Immunol. Methods 65 (1–2), 55–63.

Patel Rajesh, M., Patel, Natvar J., 2011. In vitro antioxidant activity of coumarin compounds by DPPH, Super oxide and nitric oxide free radical scavenging methods. J. Adv. Pharm. Educ. Res. 1, 52–68.

Qaisar, S., Khawaja, K.F., 2012. Cloud computing: network/security threats and countermeasures. Interdis. J. Contemp. Res. Bus. 3, 1323–1329.

Qaisar, M., NaeemuddinGilani, S., Farooq, S., 2012. Preliminary comparative phytochemical screening of euphorbia species. Am.-Eurasian J. Agric. Environ. Sci. 12 (8), 1056–1060.

Rauf, A., Khan, A., Uddin, N., Akram, M., Arfan, M., Uddin, G., et al., 2014. Preliminary phytochemical screening, antimicrobial and antioxidant activities of *Euphorbia milli*. Pakistan J. Pharm. Sci. 27 (4).

Rehman, K., Chohan, T.A., Waheed, I., Gilani, Z., Akash, M.S.H., 2019. Taxifolin prevents postprandial hyperglycemia by regulating the activity of α-amylase: evidence from an in vivo and in silico studies. J. Cell. Biochem. 120 (1), 425–438.

Rehman, K., Munawar, S.M., Akash, M.S.H., Buabeid, M.A., Chohan, T.A., Tariq, M., et al., 2020. Correction: Hesperidin improves insulin resistance via down-regulation of inflammatory responses: biochemical analysis and in silico validation. PLoS ONE 15, (2) e0229348.

Ryckaert, J.-P., Ciccotti, G., Berendsen, H.J., 1977. Numerical integration of the cartesian equations of motion of a system with constraints: molecular dynamics of n-alkanes. J. Comput. Phys. 23 (3), 327–341.

Safarzadeh, E., Shotorbani, S.S., Baradaran, B., 2014. Herbal medicine as inducers of apoptosis in cancer treatment. Adv. Pharm. Bull. 4 (Suppl 1), 421.

Salganik, R.I., 2001. The benefits and hazards of antioxidants: controlling apoptosis and other protective mechanisms in cancer patients and the human population. J. Am. Coll. Nutr. 20 (sup5), 464S–472S.

Saxena, M., Saxena, J., Nema, R., Singh, D., Gupta, A., 2013. Phytochemistry of medicinal plants. J. Pharmacogn. Phytochem. 1 (6).

Sayre, P.H., Finer-Moore, J.S., Fritz, T.A., Biermann, D., Gates, S.B., MacKellar, W.C., et al., 2001. Multi-targeted antifolates aimed at avoiding drug resistance form covalent closed inhibitory complexes with human and Escherichia coli thymidylate synthases. J. Mol. Biol. 313 (4), 813–829.

Tin, A.S., Sundar, S.N., Tran, K.Q., Park, A.H., Poindexter, K.M., Firestone, G.L., 2012. Antiproliferative effects of artemisinin on human breast cancer cells requires the downregulated expression of the E2F1 transcription factor and loss of E2F1-target cell cycle genes. Anticancer Drugs 23 (4), 370–379.

Tonoli, G., Teixeira, E., Corrêa, A., Marconcini, J., Caixeta, L., Pereira-da-Silva, M., et al., 2012. Cellulose micro/nanofibres from Eucalyptus kraft pulp: preparation and properties. Carbohydr. Polym. 89 (1), 80–88.

Uttara, B., Singh, A.V., Zamboni, P., Mahajan, R., 2009. Oxidative stress and neurodegenerative diseases: a review of upstream and downstream antioxidant therapeutic options. Curr. Neuropharmacol. 7 (1), 65–74.

Wang, S., Griffiths, G., Midgley, C.A., Barnett, A.L., Cooper, M., Grabarek, J., et al., 2010. Discovery and characterization of 2-anilino-4-(thiazol-5-yl) pyrimidine transcriptional CDK inhibitors as anticancer agents. Chem. Biol. 17 (10), 1111–1121.

Welch, W., Ruppert, J., Jain, A.N., 1996. Hammerhead: fast, fully automated docking of flexible ligands to protein binding sites. Chem. Biol. 3 (6), 449–462.

Wendorff, T.J., Schmidt, B.H., Heslop, P., Austin, C.A., Berger, J.M., 2012. The structure of DNA-bound human topoisomerase II alpha: conformational mechanisms for coordinating inter-subunit interactions with DNA cleavage. J. Mol. Biol. 424 (3–4), 109–124.

Zheng, F., Luo, Y., Wei, X., Wang, B., 2009. Non-terpenoid constituents from the seeds of Euphorbia lathyris. J. Trop. Subtrop. Bot. 17 (3), 298–301.